

CAN SOLAR NEUTRINOS BE A SERIOUS BACKGROUND IN DIRECT DARK MATTER SEARCHES?

J. D. Vergados^{(1),(2)} and H. Ejiri^{(3),(4),(5)}

⁽¹⁾*Cyprus University of Technology (CUT),*

P.O. Box 50329, 3603 Limassol, Cyprus,

⁽²⁾*Physics Department, University of Ioannina, Ioannina, GR 451 10, Greece,*

⁽³⁾*RCNP, Osaka University, Osaka, 567-0047, Japan,*

⁽⁴⁾*National Institute of Radiological Sciences, Chiba, 263-8555, Japan and*

⁽⁵⁾*Nuclear Science, Czech Technical University, Brehova, Prague, Czech Republic.*

(Dated: September 11, 2021)

The coherent contribution of all neutrons in neutrino nucleus scattering due to the neutral current is examined considering the boron solar neutrinos. These neutrinos could potentially become a source of background in the future dark matter searches aiming at nucleon cross sections in the region well below the 10^{-10} pb, i.e a few events per ton per year.

PACS numbers: 13.15.+g, 14.60Lm, 14.60Bq, 23.40.-s, 95.55.Vj, 12.15.-y.

INTRODUCTION.

The universe is observed to contain large amounts of dark matter [1, 2], and its contribution to the total energy density is estimated to be $\sim 25\%$. This non-baryonic dark matter component, responsible for the growth of cosmological perturbations through gravitational instability, has still not been detected directly. Even though there exists firm indirect evidence from the halos of dark matter in galaxies and clusters of galaxies it is essential to detect matter directly.

The possibility of direct detection, however, depends on the nature of the dark matter constituents, i.e the WIMPs (weakly interacting massive particles). Supersymmetry naturally provides candidates for these constituents [3, 4, 5, 6, 7]. In the most favored scenario of supersymmetry, the lightest supersymmetric particle (LSP) can be described as a Majorana fermion, a linear combination of the neutral components of the gauginos and higgsinos. Other possibilities also exist, see, e.g. some models in universal theories with extra dimensions [8]. Since the WIMPs are expected to be very massive ($m_{WIMP} \geq 30$ GeV) and extremely non-relativistic with average kinetic energy $\langle T \rangle \simeq 50$ keV ($m_{WIMP}/100$ GeV), a WIMP interaction with a nucleus in an underground detector is not likely to produce excitation. As a result, WIMPs can be directly detected mainly via the recoil of a nucleus (A, Z) in elastic scattering. The event rate for such a process can be computed from the following ingredients:

1. An effective Lagrangian at the elementary particle (quark) level obtained in the framework of the prevailing particle theory. For supersymmetry this is achieved as described, e. g., in refs. [6, 9]. For Kaluza Klein theories in universal extra dimensions see, e. g., some recent calculations [10]. Invariably this ingredient is the most important element, but at present, unfortunately, with the greatest uncertainty in getting the event rate, especially since the WIMP mass is quite uncertain.
2. A well defined procedure for transforming the amplitude obtained using the previous effective Lagrangian from the quark to the nucleon level, i.e. a quark model for the nucleon. This step in SUSY models is non-trivial, since the obtained results depend crucially on the content of the nucleon in quarks other than u and d.
3. Knowledge of the relevant nuclear matrix elements [11, 12], obtained with reliable many-body nuclear wave functions. Fortunately, in the case of the scalar coupling, which is viewed as the most important, the situation is a bit simpler, as only the nuclear form factor is needed.
4. Knowledge of the WIMP density in our vicinity and its velocity distribution. Since the essential input here comes from the rotation curves, dark matter candidates other than the LSP are

also characterized by similar parameters. One does not know for sure what these parameters are. The most common models are isothermal Maxwell-Boltzmann (M-B) distributions [13, 14, 15, 16], anisotropic velocity distributions described by Tsallis type functions [17, 18, 19, 20], i.e. functions which in some limit lead to the M-B distributions, and variants of the M-B distributions arising when dark matter is coupled to dark energy [21]. Non isothermal models, like those arising in the Eddington approach have also been considered [22, 23, 24, 25]. These various models give similar (time averaged) rates and differ only in the predictions regarding the modulation. So one may assume that the uncertainties in this case are quite small.

The particle physics in conjunction with the structure of the nucleon provide the nucleon cross sections. Since, as we have already mentioned, the particle physics parameters most likely will result in very small cross sections, the most ambitious future dark matter experiments like the XENON-ZEPLIN aim at detecting 10 events per ton per year. At this level one may encounter very bothersome backgrounds. One such background may come from the high energy boron solar neutrinos (the other neutrinos are characterized either by too small energy or much lower fluxes).

During the last years various detectors aiming at detecting recoiling nuclei have been developed in connection with dark matter searches [26] with thresholds in the few keV region. Recently, however, it has become feasible to detect neutrinos by measuring the recoiling nucleus and employing gaseous detectors with much lower threshold energies [27]. Thus one is able to explore the advantages offered by the neutral current interaction, exploring ideas put forward more than a decade ago [28]. Furthermore this interaction, through its vector component, can lead to coherence, i.e. an additive contribution of all neutrons in the nucleus (the vector contribution of the protons is tiny, so the coherence is mainly due to the neutrons of the nucleus).

In this paper we will derive the differential neutrino nucleus cross section and the associated event rate for the elastic (coherent) neutrino-nucleus scattering. Then we will utilize the available information regarding the energy spectrum of solar boron neutrinos and estimate the expected number of events for light as well as heavy nuclear target. Finally we will compare the recoil spectrum and total event rate associated with WIMPs with that due to neutrinos.

A BRIEF DISCUSSION OF THE RATES FOR DIRECT WIMP DETECTION

Before proceeding with the evaluation of the event rate for nuclear recoils originating from the neutrino nuclear scattering we will briefly discuss the WIMP-nucleus recoiling events. We begin by saying that the shape of the differential event rate for WIMP detection cannot be precisely estimated, since, as we mentioned in the introduction, the WIMP-nucleon cross section is not known. Especially its dependence on the WIMP mass is not known. The non-directional differential rate folded with the WIMP velocity distribution is given by [29, 30, 31, 32]:

$$\left\langle \frac{dR}{du} \right\rangle = \frac{\rho(0)}{m_\chi} \frac{m}{Am_N} \sqrt{\langle v^2 \rangle} \int \frac{|v|}{\sqrt{\langle v^2 \rangle}} f(\mathbf{v}, \mathbf{v}_E) \frac{d\sigma(u, v)}{du} d^3\mathbf{v} \quad (1)$$

where $f(\mathbf{v}, \mathbf{v}_E)$ essentially is the WIMP velocity distribution in the laboratory frame with \mathbf{v}_E the velocity of the Earth.

The differential cross section is given by:

$$d\sigma(u, v) = \frac{du}{2(\mu_r b v)^2} [(\bar{\Sigma}_S F(u))^2 + \bar{\Sigma}_{spin} F_{11}(u)] \quad (2)$$

where u the energy transfer Q in dimensionless units given by

$$u = \frac{Q}{Q_0}, \quad Q_0 = [m_p A b]^{-2} = 40 A^{-4/3} \text{ MeV} \quad (3)$$

with b is the nuclear (harmonic oscillator) size parameter. $F(u)$ is the nuclear form factor and $F_{11}(u)$ is the spin response function associated with the isovector channel.

The scalar cross section is given by:

$$\bar{\Sigma}_S = \left(\frac{\mu_r(A)}{\mu_r(p)}\right)^2 \sigma_{p,\chi^0}^S A^2 \left[\frac{1 + \frac{f_S^1}{f_S^0} \frac{2Z-A}{A}}{1 + \frac{f_S^1}{f_S^0}} \right]^2 \approx \sigma_{N,\chi^0}^S \left(\frac{\mu_r(A)}{\mu_r(p)}\right)^2 A^2 \quad (4)$$

(since the heavy quarks dominate the isovector contribution is negligible). σ_{N,χ^0}^S is the LSP-nucleon scalar cross section. The spin cross section is given by:

$$\bar{\Sigma}_{spin} = \left(\frac{\mu_r(A)}{\mu_r(p)}\right)^2 \sigma_{p,\chi^0}^{spin} \zeta_{spin} \quad (5)$$

ζ_{spin} the nuclear spin ME.

Integrating over the energy transfer u we obtain the event rate for the coherent WIMP-nucleus elastic scattering, which is given by [29, 30, 31, 32]:

$$R = \frac{\rho(0)}{m_{\chi^0}} \frac{m}{m_p} \sqrt{\langle v^2 \rangle} \left[f_{coh}(A, \mu_r(A)) \sigma_{p,\chi^0}^S + f_{spin}(A, \mu_r(A)) \sigma_{p,\chi^0}^{spin} \zeta_{spin} \right] \quad (6)$$

with

$$f_{coh}(A, \mu_r(A)) = \frac{100\text{GeV}}{m_{\chi^0}} \left[\frac{\mu_r(A)}{\mu_r(p)} \right]^2 A t_{coh} (1 + h_{coh} \cos\alpha) \quad (7)$$

$$f_{spin}(A, \mu_r(A)) = \left[\frac{\mu_r(A)}{\mu_r(p)} \right]^2 \frac{t_{spin}(A)}{A} \quad (8)$$

In this work we will not be concerned with the spin cross section. The parameter t_{coh} takes into account the folding of the nuclear form factor with the WIMP velocity distribution, h_{coh} deals with the modulation due to the motion of the Earth and α is the phase of the Earth (zero around June 2nd).

The number of events in time t due to the scalar interaction, which leads to coherence [21], is:

$$R \simeq 1.60 \cdot 10^{-3} \times \frac{t}{1\text{y}} \frac{\rho(0)}{0.3\text{GeVcm}^{-3}} \frac{m}{1\text{Kg}} \frac{\sqrt{\langle v^2 \rangle}}{280\text{km s}^{-1}} \frac{\sigma_{p,\chi^0}^S}{10^{-6} \text{pb}} f_{coh}(A, \mu_r(A)) \quad (9)$$

Assuming a constant nucleon cross section we get the differential rate indicated by Figs 1 and 2. This shape was obtained in the coherent mode, but we expect to have a similar shape due to the spin [29, 33]. The essential difference is that one needs as input a much larger nucleon cross section due to the spin. Indeed for a heavy target the spin mode has no chance, if the nucleon cross section due to the spin is of the same magnitude with that associated with the coherent mode.

The total (time averaged) coherent event rate is shown in Figs 5 and 8.

ELASTIC NEUTRINO NUCLEON SCATTERING

The cross section for elastic neutrino nucleon scattering has extensively been studied. It has been shown that at low energies it can be simplified and be cast in the form: [34],[35]:

$$\left(\frac{d\sigma}{dT_N} \right)_{weak} = \frac{G_F^2 m_N}{2\pi} [(g_V + g_A)^2 + (g_V - g_A)^2 \left[1 - \frac{T_N}{E_\nu} \right]^2 + (g_A^2 - g_V^2) \frac{m_N T_N}{E_\nu^2}] \quad (10)$$

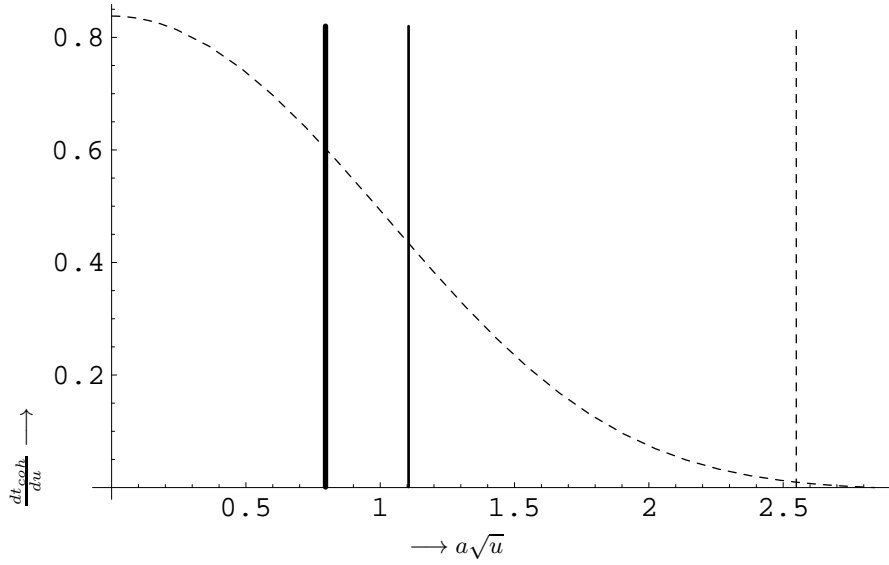


FIG. 1: The differential event rate for the coherent process, in arbitrary units, as a function of the parameter $a\sqrt{u}$, where $a = 1.410^{-3}(\mu_r(A)c^2b/(\hbar c))$ with $\mu_r(A)$ the WIMP-nucleus reduced mass and b the size parameter for the nucleus. u is essentially the energy transfer Q , $u = Q/Q_0$, $Q_0 = 4.110^4 A^{-4/3}$. Due to the nuclear form factor not all the range of u is exploitable in direct WIMP detection. For ^{131}Xe , e.g., effectively there is an upper cut off value indicated by dotted line, fine line and thick line for a WIMP mass of 30, 100 and 200 GeV respectively. Any lower cut off is due to the threshold.

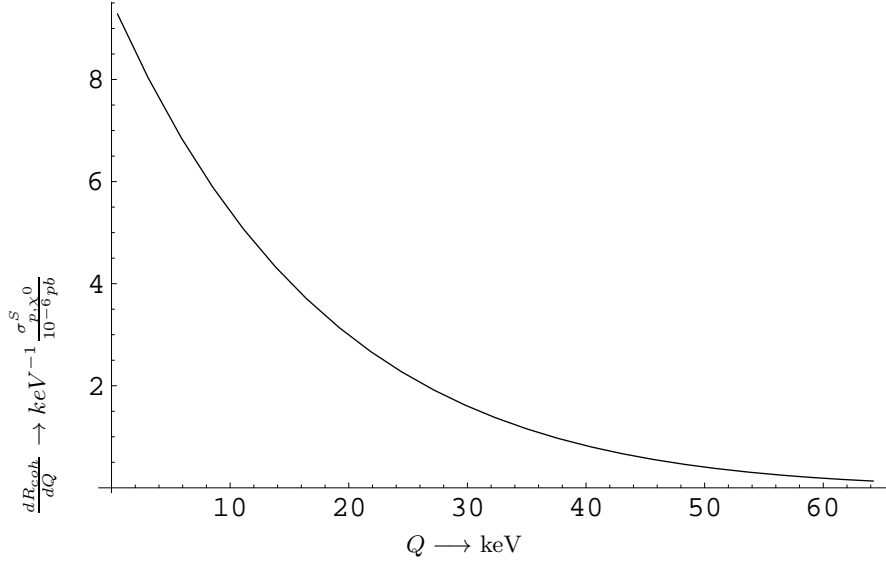


FIG. 2: We show the differential event rate dR_{coh}/dQ for the coherent process, as a function of the energy transfer, for a WIMP mass, m_χ , of 100 GeV in the case of ^{131}Xe .

where m_N is the nucleon mass and g_V , g_A are the weak coupling constants. Neglecting their dependence on the momentum transfer to the nucleon they take the form:

$$g_V = -2 \sin^2 \theta_W + 1/2 \approx 0.04, \quad g_A = \frac{1.27}{2}, \quad (\nu, p) \quad (11)$$

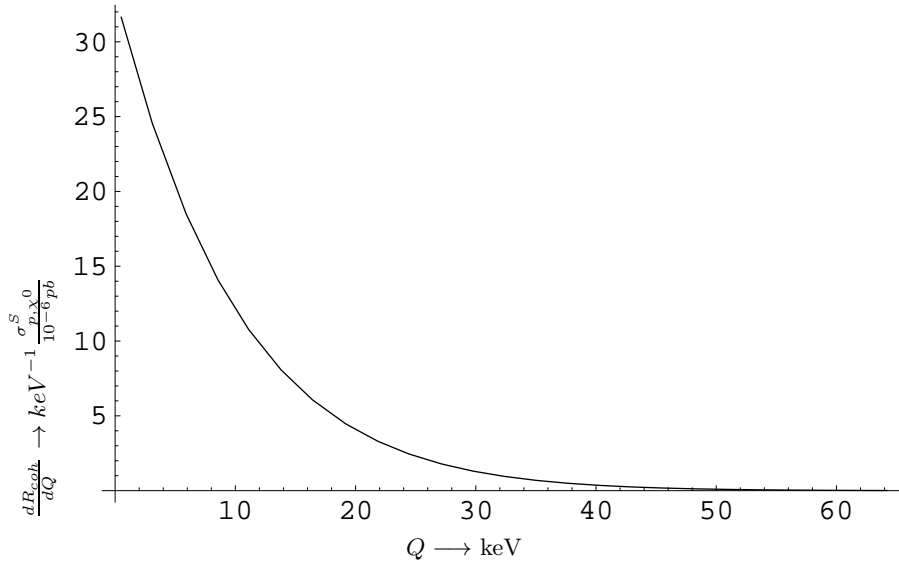


FIG. 3: The same as in Fig. 2 a WIMP mass of 30 GeV.

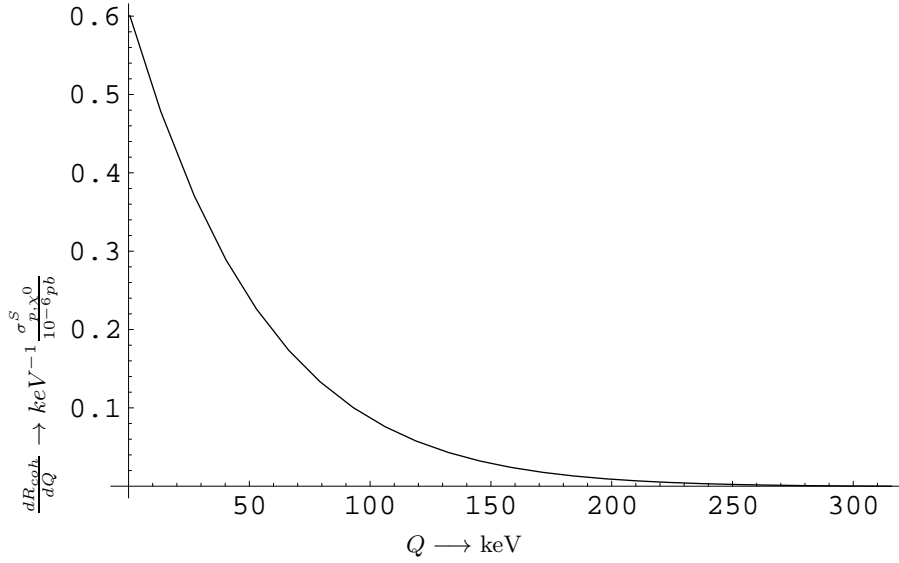


FIG. 4: The same as in Fig. 2 in the case of the A=32 target.

$$g_V = -1/2, \quad g_A = -\frac{1.27}{2}, \quad (\nu, n) \quad (12)$$

In the above expressions for the axial current the renormalization in going from the quark to the nucleon level was taken into account. For antineutrinos $g_A \rightarrow -g_A$. To set the scale we write:

$$\frac{G_F^2 m_N}{2\pi} = 5.14 \times 10^{-41} \frac{\text{cm}^2}{\text{MeV}} \quad (13)$$

The nucleon energy depends on the neutrino energy and the scattering angle, the angle between the direction of the recoiling particle and that of the incident neutrino. In the laboratory frame it is

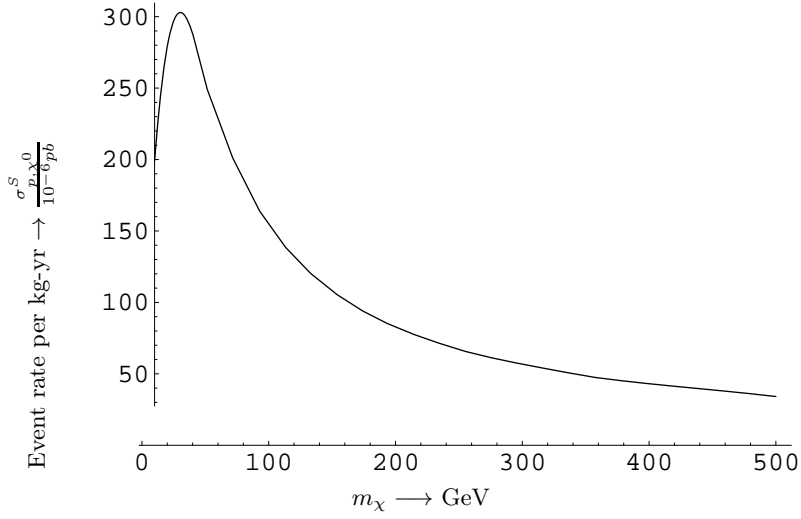


FIG. 5: We show the total event rate for the coherent process as a function of the WIMP mass in the case of ^{131}Xe for zero threshold.

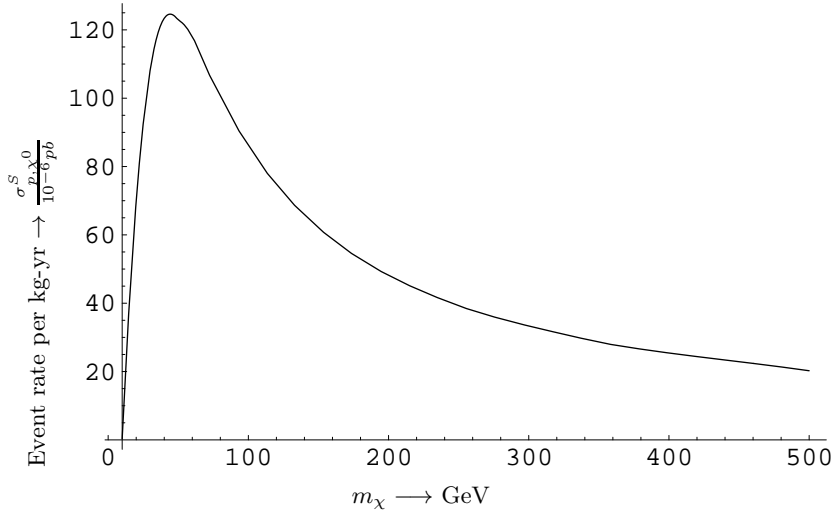


FIG. 6: The same as in Fig. 5 for a detector energy threshold of 10 keV.

given by:

$$T_N = \frac{2 m_N (E_\nu \cos \theta)^2}{(m_N + E_\nu)^2 - (E_\nu \cos \theta)^2} \quad , \quad 0 \leq \theta \leq \pi/2 \quad (14)$$

(forward scattering). For sufficiently small neutrino energies, the last equation can be simplified as follows:

$$T_N \approx \frac{2(E_\nu \cos \theta)^2}{m_N}$$

The above formula can be generalized to any target and can be written in dimensionless form as follows:

$$y = \frac{2 \cos^2 \theta}{(1 + 1/x_\nu)^2 - \cos^2 \theta} \quad , \quad y = \frac{T_{recoil}}{m_{recoil}} \quad , \quad x_\nu = \frac{E_\nu}{m_{recoil}} \quad (15)$$

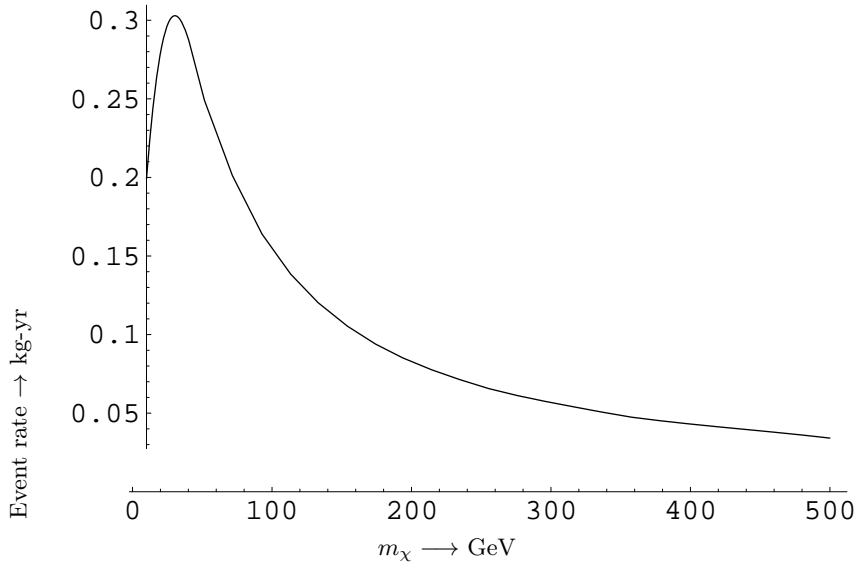


FIG. 7: We show the total event rate for the coherent process as a function of the WIMP mass in the case of ^{131}Xe , employing a nucleon cross section of $\sigma_{p,\chi^0}^S = 10^{-9}pb$.

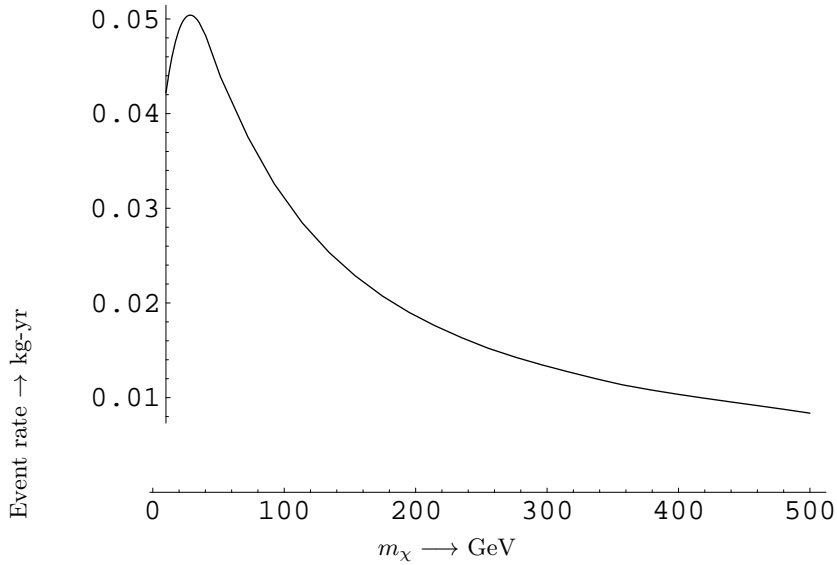


FIG. 8: The same as in Fig. 7 in the case of the A=32 system.

In the present calculation we will treat x_ν and y as dynamical variables, in line with CDM recoils. One, of course, equally well could have chosen x_ν and θ as relevant variables.

The maximum energy occurs when $\theta = 0$, i.e.:

$$y_{max} = \frac{2}{(1 + 1/x_\nu)^2 - 1}, \quad (16)$$

in agreement with Eq. (2.5) of ref. [34]. One can invert Eq. 15 and get the neutrino energy associated with a given recoil energy and scattering angle. One finds

$$x_\nu = \left[-1 + \cos\theta \sqrt{1 + \frac{2}{y}} \right]^{-1}, \quad 0 \leq \theta \leq \pi/2 \quad (17)$$

The minimum neutrino energy for a given recoil energy is given by:

$$x_\nu^{min} = \left[-1 + \sqrt{1 + \frac{2}{y}} \right]^{-1} = \frac{y}{2} \left(1 + \sqrt{1 + \frac{2}{y}} \right) \quad (18)$$

in agreement with Eq. (4.2) of ref. [34]. The last equation is useful in obtaining the differential cross section (with respect to the recoil energy) after folding with the neutrino spectrum

COHERENT NEUTRINO NUCLEUS SCATTERING

From the above expressions we see that the vector current contribution, which may lead to coherence, is negligible in the case of the protons. Thus the coherent contribution [36] may come from the neutrons and is expected to be proportional to the square of the neutron number. The neutrino-nucleus scattering can be derived in analogous fashion. It can also be obtained from the amplitude of the neutrino nucleon scattering by employing the appropriate kinematics, i.e. those involving the elastically scattered nucleus and the substitution

$$\mathbf{q} \Rightarrow \frac{\mathbf{p}}{A} \quad , \quad E_N \Rightarrow \sqrt{m_N^2 + \frac{\mathbf{p}^2}{A^2}} = \frac{E_A}{A}$$

with \mathbf{q} the nucleon momentum and \mathbf{p} the nuclear momentum. Under the above assumptions the neutrino-nucleus cross section takes the form:

$$\begin{aligned} \left(\frac{d\sigma}{dT_A} \right) &= \frac{G_F^2 Am_N}{2\pi} [(M_V + M_A)^2 \left(1 + \frac{T_A}{E_\nu} \right) \\ &+ (M_V - M_A)^2 \left(1 - \frac{T_A}{E_\nu} \right)^2 + (M_A^2 - M_V^2) \frac{Am_N T_A}{E_\nu^2}] \end{aligned} \quad (19)$$

where M_V and M_A are the nuclear matrix elements associated with the vector and the axial currents respectively and T_A is the energy of the recoiling nucleus. The axial current contribution vanishes for $0^+ \Rightarrow 0^+$ transitions. Anyway it is negligible in front of the coherent scattering due to neutrons. Thus the previous formula is reduced to:

$$\left(\frac{d\sigma}{dT_A} \right)_{weak} = \frac{G_F^2 Am_N}{2\pi} (N^2/4) F_{coh}(T_A, E_\nu), \quad (20)$$

with

$$F_{coh}(T_A, E_\nu) = F^2(q^2) \left(1 + \left(1 - \frac{T_A}{E_\nu} \right)^2 - \frac{Am_N T_A}{E_\nu^2} \right) \quad (21)$$

where $F(q^2) = F(T_A^2 + 2Am_N T_A)$ is the nuclear form factor.

The nuclear form factor makes a sizable contribution in the case of the more energetic supernova neutrinos. In the case of solar neutrinos, due to the small nuclear recoil energy, the form factor is expected to play a minor role numerically.

By setting the form factor equal to unity in F_{coh} we obtain f_{coh} . The latter is shown in Fig. 9. Note that the maximum recoil energy for boron neutrinos cannot exceed the 4 keV in the case of Xe and 17 keV in the case of S. The differential cross section is shown in Figs 12 and 13. Note the rapid fall of the cross section with recoil energy. The cross section has been almost completely depleted beyond energies 1 and 5 keV for a intermediate (^{131}Xe) and light (^{32}S) targets respectively.

THE EVENT RATE

To proceed further we must convolute the cross section with the neutrino spectrum. From the neutrinos emitted by the sun only the boron neutrinos have high enough flux with sufficiently

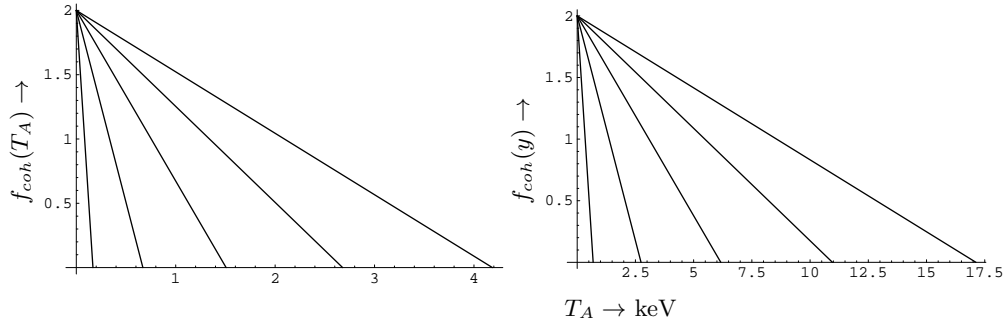


FIG. 9: The function $f_{coh}(T_A)$, obtained from $F_{coh}(T_A)$ after setting the form factor and the quenching factor equal to unity, for $A=131$ on the left and $A=32$ on the right as a function of the recoil energy (for neutrino energies 3, 6, 9, 12 and 15 keV increasing to the right). According to Eq. (16) the maximum recoil energy is increasing as the neutrino energy increases.

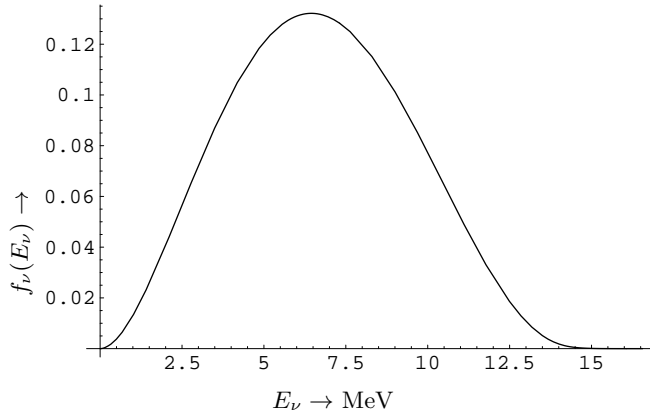


FIG. 10: The boron solar neutrino spectrum.

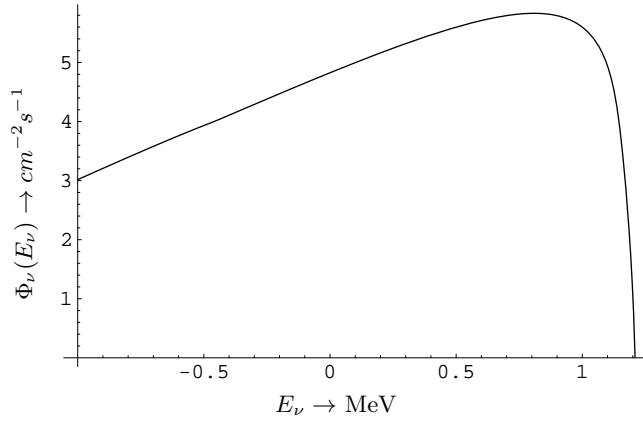


FIG. 11: The boron solar neutrino flux in units of $cm^{-2}s^{-1}$ in a Log-Log plot.

high energy to lead to nuclear recoils, which could become relevant in dark matter searches. The normalized boron neutrino spectrum is shown in Fig. 10. The corresponding flux is shown in Fig. 11. The obtained differential cross section is shown in Figs 12 and 13.

Integrating the differential cross section down to zero threshold we find the event rates given

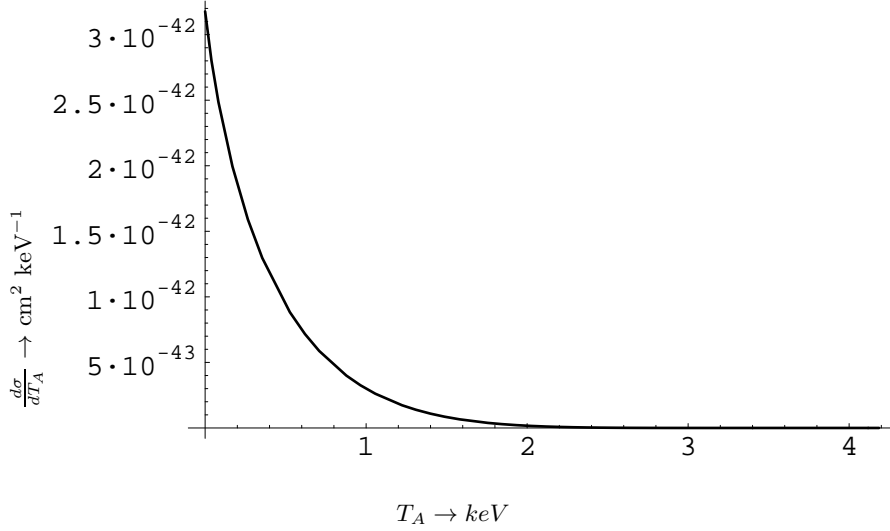


FIG. 12: The neutrino induced differential cross section in units $\text{cm}^2 \text{keV}^{-1}$ as a function of the recoil energy in keV in the case of the target ^{131}Xe . Note that essentially all the contribution comes from the recoil energy region $0 \leq T_A \leq 1$ keV. The effect of the form factor is invisible in the figure.

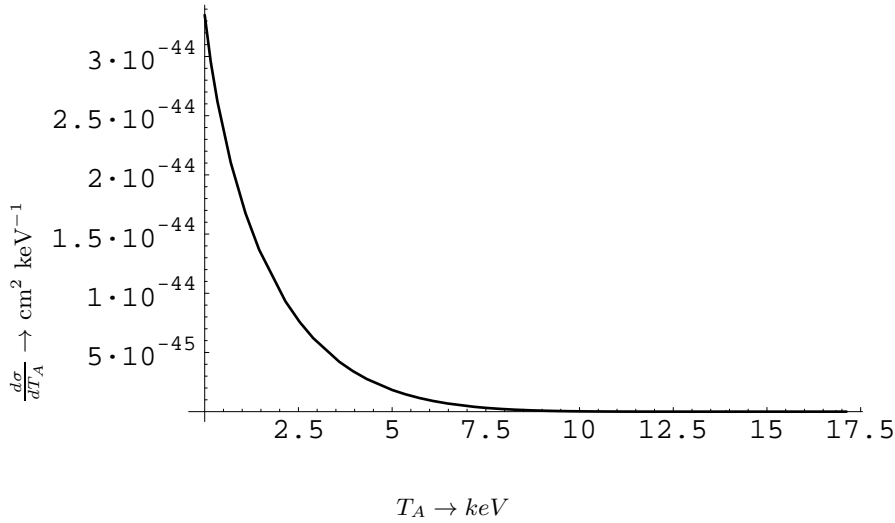


FIG. 13: The same as in Fig. 12 for the target ^{32}S . In this case the recoil energy region is wider $0 \leq T_A \leq 5$ keV, but still small.

in table I. The event rates are almost two orders of magnitude smaller than the rates for WIMP detection obtained with a nucleon cross section of 10^{-9}pb . Thus such neutrinos cannot be a serious background for WIMP searches in the region $10^{-9} - 10^{-10}\text{pb}$. In any event, as we will see below, the neutrino induced recoils are less of a background problem in the realistic case of non zero energy threshold.

Sometimes for experimental purposes one may have to focus on a restricted region of the recoil energy spectrum. To be specific let us consider a typical low recoil energy region, e.g. $2 \text{keV} \leq T_A \leq 4 \text{keV}$. Clearly from Fig. 12 one can see that the neutrino background is very small in this energy region.

TABLE I: Comparison of the event rates for boron solar neutrino detection with those of WIMP detection rates. In evaluating the latter we assumed a nucleon cross section independent of the mass. The kinematics were obtained assuming two WIMP masses, namely 100 and 300 GeV. NoFF means that the nuclear form factor was neglected.

	target	$R_\chi(\text{kg}\cdot\text{y}) \times \frac{\sigma_N}{10^{-9}\text{pb}}$ $m_\chi = 100\text{GeV}$	$R_\chi(\text{kg}\cdot\text{y}) \times \frac{\sigma_N}{10^{-9}\text{pb}}$ $m_\chi = 300\text{GeV}$	$R_\nu(\text{kg}\cdot\text{y})$	$R_\nu(\text{kg}\cdot\text{y});\text{NoFF}$
full range	^{131}Xe	0.167	0.060	0.934×10^{-3}	0.952×10^{-3}
	^{32}S	0.033	0.014	0.167×10^{-3}	0.168×10^{-3}
$2\text{keV} \leq T_A \leq 4\text{keV}$	^{131}Xe	0.018	0.010	0.308×10^{-5}	0.310×10^{-5}
	^{32}S	0.0012	0.0006	0.367×10^{-4}	0.368×10^{-4}

We find that the WIMP event rate in this restricted energy region is substantially reduced, but it is not suppressed as much as the neutrino rate (see table I).

We should mention that the obtained rates are independent of the neutrino oscillation parameters, since the neutral current events, which we considered in the present calculation, are not affected by such oscillations.

QUENCHING FACTORS AND ENERGY THRESHOLDS

. The above results refer to an ideal detector operating down to zero energy threshold. For a real detector, however, as we have already mentioned, the nuclear recoil events are quenched, especially at low energies. The quenching factor for a given detector is the ratio of the signal height for a recoil track divided by that of an electron signal height with the same energy. We should not forget that the signal heights depend on the velocity and how the signals are extracted experimentally. The actual quenching factors must be determined experimentally for each target. In the case of NaI the quenching factor is 0.05, while for Ge and Si it is 0.2-0.3. For our purposes it is adequate, to multiply the energy scale by an recoil energy dependent quenching factor, $Q_{fac}(T_A)$ adequately described by the Lidhard theory [37]. More specifically in our estimate of $Qu(T_A)$ we assumed a quenching factor of the following empirical form [38]-[37]:

$$Q_{fac}(T_A) = r_1 \left[\frac{T_A}{1\text{keV}} \right]^{r_2}, \quad r_1 \simeq 0.256, \quad r_2 \simeq 0.153 \quad (22)$$

The quenching factors very much depend on the detector type. The quenching factor, exhibited in Figs 14 and 15 for recoil energies of ^{131}Xe and ^{32}S respectively, were obtained assuming the same quenching of the form of Eq. (22). In the presence of the quenching factor as given by Eq. (22) the measured recoil energy is typically reduced by factors of about 3, when compared with the electron energy. In other words a threshold energy of electrons of 1 keV becomes 3 keV for nuclear recoils. Accordingly, the event rates for neutrino recoils are reduced much, as seen from Figs 16 and 17 below. On the other hand the WIMP recoil events are not reduced much, since the recoil energy is well above threshold.

The above rates were obtained in the case of zero threshold. Due to the relatively low recoil energies,

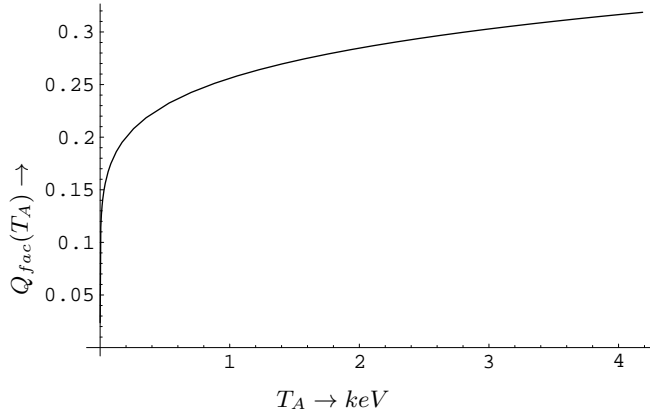


FIG. 14: The quenching factor in the case of $A=131$ as a function of the recoil energy.

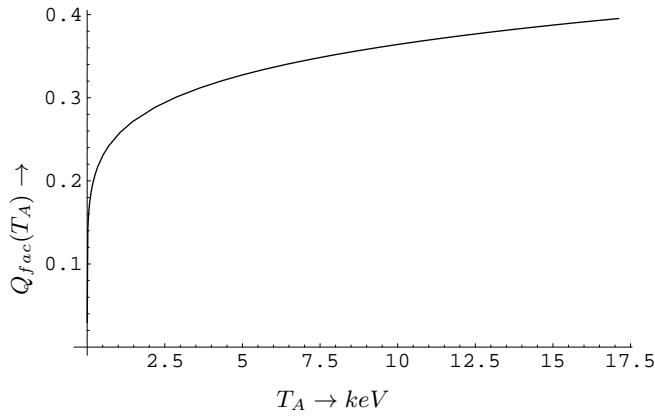


FIG. 15: The quenching factor in the case of $A=32$ as a function of the recoil energy. It is similar to Fig. 14 except that the allowed recoil energy is different.

however, the effect of threshold is crucial (see Figs 16 and 17). One clearly sees that the observed events are an order of magnitude down if the energy threshold is 1 keV (2 keV) for Xe(S) respectively. Thus with quenching most signals get below the threshold energy of ≈ 1 keV. On the other hand the WIMP event rates are almost unaffected, unless the threshold energy becomes larger than 5 keV.

CONCLUDING REMARKS

In the present study we considered the elastic scattering of WIMP-nucleus interaction and the corresponding elastic scattering of boron solar neutrinos. The former are favored by an A^2 enhancement due to coherence of all nucleons, while the latter by N^2 due to the neutron coherence resulting from the neutral current interaction. The latter may become a source of background, if the WIMP nucleon interaction turns out to be very small. Our results can be summarized as follows:

1. The differential cross section for solar neutrinos decreases sharply as the nuclear recoil energy increases. It almost vanishes beyond 1 keV (5 keV) for intermediate (light target), like ^{131}Xe (^{32}S). On the other the corresponding event rates for WIMPs of mass ≈ 100 GeV extend further than 30 (150) keV ^{131}Xe (^{32}S) respectively.
2. The event rates for boron solar neutrinos at zero threshold energy and no quenching are 2-

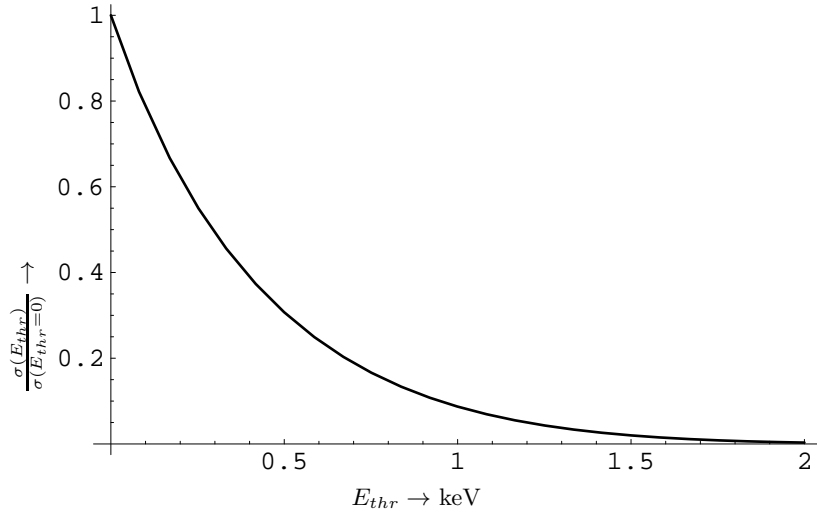


FIG. 16: The ratio of the total cross section with threshold divided by that with zero threshold for $A=131$ as a function of the threshold energy. Otherwise the notation is similar to that of Fig. 12. Note that the observed events are an order of magnitude down, if the energy threshold is 1 keV.

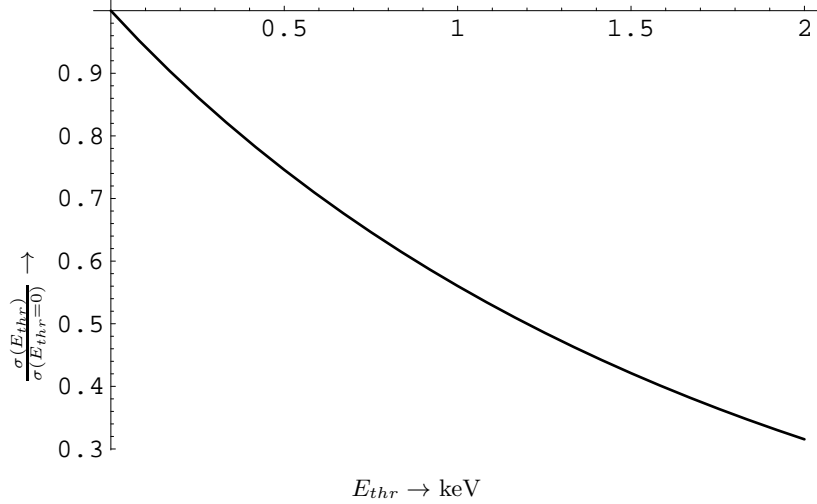


FIG. 17: The ratio of the total cross section with threshold divided by that with zero threshold for $A=32$ as a function of the threshold energy. Otherwise the notation is similar to that of Fig. 16. Note that the observed events are an order of magnitude down, if the energy threshold is above 2 keV.

3 orders of magnitude smaller than those for WIMPs with a nucleon cross section 10^{-9} pb. Thus solar neutrinos are not a serious background down to 10^{-10} pb, but they may have to be considered at the level of 10^{-11} pb.

3. Since the nuclear recoil energy arising from solar neutrino scattering is smaller than that associated with heavy WIMPs, one can further substantially decrease its contribution by restricting the observation of the recoil energy spectra above a few keV without seriously affecting the corresponding WIMP rates. Thus neutrinos do not appear to be a serious background even at the level of 10^{-11} pb.
4. By exploiting the quenching factors one may reduce this background still further.

5. It should be noted that the solar neutrinos do not affect the DAMA result, *Bernabei et al* [26], in both the energy and the cross section. DAMA uses the NaI target with a large quenching factor. Since events from NaI are mostly due to ^{127}I , the event rate and the quenching factor are nearly the same as those for ^{131}Xe discussed in the text. Thus the solar neutrino events are below 1 keV, i.e. they are below the DAMA energy bin 2-4 keV. In other words the solar neutrinos may be dangerous for WIMP detection for WIMP-nucleon cross section less than 10^{-10} pb, which is far below the DAMA region of $10^{-5} - 10^{-6}$ pb.
6. The observation of the annual modulation of the signal (see e.g. [30] and references there in) or even better by performing directional experiments [39],[40], i.e experiments in which the direction of recoil is also measured, one will be able to select WIMP signals and discriminate against neutrino scattering.

In the above discussion we focused on the coherent WIMP-nucleus scattering. We should not, of course, forget the spin contribution due to the axial current. In this case one has to deal with the proton and neutron spin nuclear matrix elements and the relevant elementary proton and neutron spin amplitudes. So the obtained results will depend on the specific target. It is clear, however, that the spin matrix elements do not exhibit coherence, i.e. do not scale with A^2 . Thus the event rates will be suppressed. In other words the boron neutrinos maybe be a serious background for nucleon spin cross section at the level of 10^{-8} pb. This, of course, will be worrisome, but then the corresponding coherent cross section must be less than 10^{-11} pb, since it is only then that the two modes can compete.

ACKNOWLEDGMENTS

One of us (JDV) is indebted to professor Pantelis Kelires and the Cyprus Technical University for their hospitality and support. Partial financial support by MRTN-CT-2004-503369 and MRTN-CT-2006-035863 is also acknowledged. The other author (H.E.) thanks the NIRS directors and the NIRS colleagues for their support and hospitality at NIRS.

-
- [1] D.N. Spergel *et al*, Three-Year WMAP Results: Implications for Cosmology, astro-ph/0603449; L. Page *et al*, Three-Year WMAP Results: Polarization Analysis, astro-ph/0603450; G. Hinsaw *et al*, Three-Year WMAP Observations: Implications Temperature Analysis, astro-ph/0603451; N Jarosik *et al*, Three-Year WMAP Observations: Beam Profiles, Data Processing, Radiometer Characterization and Systematic Error Limits, astro-ph/0603452.
 - [2] D.N. Spergel *et al*, *Astrophys. J. Suppl.* **148**, 175 (2003).
 - [3] M. W. Goodman and E. Witten, *Phys. Rev. D* **31**, 3059 (1985).
 - [4] T. S. Kosmas and J. D. Vergados, *Phys. Rev. D* **55**, 1752 (1997).
 - [5] J. Ellis and L. Roszkowski, *Phys. Lett. B* **283**, 252 (1992).
 - [6] A. Bottino *et al.*, *Phys. Lett B* **402**, 113 (1997).
R. Arnowitt. and P. Nath, *Phys. Rev. Lett.* **74**, 4592 (1995); *Phys. Rev. D* **54**, 2374 (1996); hep-ph/9902237;
V. A. Bednyakov, H.V. Klapdor-Kleingrothaus and S.G. Kovalenko, *Phys. Lett. B* **329**, 5 (1994).
 - [7] Update on the Direct Detection of Supersymmetric Dark Matter J. Ellis, K. A. Olive, Y. Santoso, V. C. Spanos, hep-ph/0502001.
 - [8] See, e.g., G. Servant, in Les Houches :Physics at TeV Colliders 2005” Beyond the Standard Model working group: summary report, B.C. Allanach (ed.), C. Grojean (ed.), P. Skands (ed.), *al*, section 25, p.164; hep-ph/0602198.
 - [9] J. D. Vergados, *J. of Phys. G* **22**, 253 (1996).
 - [10] V. Oikonomou, J. Vergados, and C. C. Moustakidis, *Nuc. Phys.* **B 773**, 19 (2007).
 - [11] M. T. Ressel *et al.*, *Phys. Rev. D* **48**, 5519 (1993); M.T. Ressel and D. J. Dean, *Phys. Rev. C* **56**, 535 (1997).
 - [12] P. C. Divari, T. S. Kosmas, J. D. Vergados, and L. D. Skouras, *Phys. Rev. C* **61**, 054612 (2000).

- [13] A. K. Drukier, K. Freeze and D. N. Spergel, *Phys. Rev. D*, **33**, 3495 (1986);
J.I. Collar et al., *Phys. Lett B* **275**, 181 (1992).
- [14] J. D. Vergados, *Phys. Rev. D* **62**, 023519 (2000).
- [15] N. Forengo and S. Scopel, *Phys. Lett. B* **576**, 189 (2003).
- [16] N. Evans, M. Carollo, and P. Zeeuw, *Mon. Not. R. Astron. Soc* **318**, 1131 (2000).
- [17] S. Hansen, B. Moore, M. Zemp, and J. Stadel, *J. Cosmol. Astropart. Phys.* **0601**, 014 (2006).
- [18] O. Host and S. Hansen, *J. Cosmol. Astropart. Phys.* **0601**, 016 (2007).
- [19] S.H. Hansen, R. Piffaretti, arxiv:0705:4680.
- [20] J. Vergados, S. N. Hansen, and O. Host, *Phys. Rev. D* **77**, 023509 (2008).
- [21] N. Tetradis, J. Vergados, and A. Faessler, *Phys. Rev. D* **75**, 023504 (2007).
- [22] A. S. Eddington, *NRAS* **76**, 572 (1916).
- [23] P. Ullio and M. Kamiokowski, *JHEP* **0103**, 049 (2001).
- [24] J. Vergados and D. Owen, *Phys. Rev. D* **75**, 043503 (2007).
- [25] P. Belli, R. Cerulli, N. Fornego, and S. Scopel, *Phys. Rev. D* **66**, 043503 (2002).
- [26] See, e.g,
R. Bernabei et al., *Phys. Lett. B* **389** (1996) 757 . R. Bernabei et al., *Phys. Lett. B* **424** (1998) 195;
B 450 448 (1999) 448.
A. Benoit *et al*, [EDELWEISS collaboration], *Phys. Lett. B* **545** 43 (2002) 43; V. Sanglard *et al* [EDELWEISS collaboration], *Phys. Rev. D* **71** (2005) 122002.
D.S. Akerib *et al*, [CDMS Collaboration], *Phys. Rev D* **68** (2003) 082002 ;arXiv:astro-ph/0405033.
G. Alner *et al*, (UK Dark Matter Collaboration), *Astropar. Physics* **23** (2005) 444.
- [27] Y. Giomataris and J. Vergados, *Phys. Lett. B* **634**, 23 (2006), ; hep-ex/0503029.
- [28] A. Burrows, D. Klein, and R. Gandhi, *Phys. Rev. D* **45**, 3361 (1992).
- [29] J. D. Vergados, *J.Phys. G* **30**, 1127 (2004), 0406134.
- [30] J. D. Vergados, *Phys. Rev. D* **57**, 103003 (2003), hep-ph/0303231.
- [31] J. D. Vergados, *Phys. Rev. D* **63**, 06351 (2001).
- [32] J. D. Vergados, On The Direct Detection of Dark Matter- Exploring all the signatures of the neutralino-nucleus interaction, hep-ph/0601064.
- [33] The Strange Spin of the Nucleon, J. Ellis and M. Karliner, hep-ph/9501280.
- [34] J. Beacom, W. Farr, and P. Vogel, *Phys. Rev. D* **66**, 03301 (2002).
- [35] P. Vogel and J. Engel, *Phys. Rev. D* **39**, 3378 (1989).
- [36] E.A. Paschos, A. Kartavtsev, hep-ph/0309148.
- [37] J. Lidhart *et al*, *Mat. Phys. Medd. Dan. Vid. Selsk*, 33 (1963) 1.
- [38] E. Simon, et al, *Nucl. Instr. Meth. A* **507**, 643 (2003).
- [39] The NAIAD experiment B. Ahmed *et al*, *Astropart. Phys.* **19** (2003) 691; hep-ex/0301039
B. Morgan, A. M. Green and N. J. C. Spooner, *Phys. Rev. D* **71** (2005) 103507; astro-ph/0408047.
- [40] J. Vergados and A. Faessler, *Phys. Rev. D* **75**, 055007 (2007).